TISSUE ENGINEERING: Part A
Volume 21, Numbers 1 and 2, 2015
DOI: 10.1089/ten.tea.2014.0003

Regenerative Potential of Low-Concentration SDS-Decellularized Porcine Aortic Valved Conduits *In Vivo*

José Rodolfo Paniagua Gutierrez, MD,[1,2] Helen Berry, PhD,[1] Sotirios Korossis, PhD,[3] Saeed Mirsadraee, PhD,[1,2] Sergio Veiga Lopes, MD,[4] Francisco da Costa, MD,[4] John Kearney, PhD,[5] Kevin Watterson, MD,[1] John Fisher, PhD,[3] and Eileen Ingham, PhD[1]

The aims of this study were to determine the functional biocompatibility of low-concentration SDS-decellularized porcine aortic roots *in vivo*. A previously developed process was modified for 9- and 15-mm-diameter aortic roots to facilitate implantation into the porcine abdominal aorta ($n = 3$) and juvenile sheep right ventricular outflow tract ($n = 7$), respectively. Native allogeneic aortic roots were used as controls. Acellular porcine roots explanted from pigs at weeks were largely repopulated with stromal cells of appropriate phenotype, and there was evidence that macrophages were involved in the regenerative process. Native allogeneic roots were subject to a classic allograft rejection response. Acellular porcine roots explanted from sheep at 6 months showed evidence of appropriate cellular repopulation, again with evidence of a role for macrophages in the regenerative process. There was some degree of calcification of two of the explanted acellular roots, likely due to incomplete removal of DNA before implantation. Native allogeneic ovine roots were subject to a classic allograft rejection response involving T cells, which resulted in overtly calcified and damaged tissues. The study highlighted (1) the importance of removal of DNA from acellular porcine valved roots to avoid calcification and (2) a role for macrophages in the regeneration of low-concentration SDS-decellularized aortic roots, as has been reported for other acellular biological extracellular matrix scaffolds.

Introduction

The most critical and most prone to failure of the four heart valves is the aortic valve. Current aortic valve replacements all have limitations.[1,2] Cryopreserved aortic valve allografts have satisfactory clinical outcomes in selected patients,[3] however, they suffer structural deterioration and have a limited lifespan in pediatric cases, associated with the generation of antibodies to donor histocompatibility antigens.[4,5] The pulmonary autograft switch operation (Ross procedure) is the only clinical procedure that provides a living functional aortic valve. The cryopreserved allograft used to replace the pulmonary valve will, however, suffer stenosis over time.[6,7]

The lack of an ideal valve replacement, together with an understanding that the immune response is a significant component of allograft valve degeneration,[8] has led to the development and clinical use of acellular allogeneic heart valves. Elkins *et al.*[9] were the first to report early clinical results of pulmonary allografts treated by the SynerGraft™ process (CryoLife).[10,11] The CryoValve SG™ pulmonary valve has been reported to perform well clinically in the short- to mid-term.[12–17] There has been one report on good results at 1 year for CryoValve SG aortic valves[18] in a small group of adults. Acellular allografts produced using different processes have also been used clinically,[19–21,22] with good results for both pulmonary valves[21] at 4 years and aortic valves at 19 months,[22] for valves decellularized using low-concentration SDS.

Despite these advances, acellular allografts still suffer from limitations of availability, particularly in sizes suitable for children. An ideal solution would be aortic valves, or pulmonary valves for the Ross procedure, available off the shelf in a range of sizes. Hence, several groups have pursued research and development of acellular porcine valves. CryoLife applied the SynerGraft process to porcine pulmonary valves and preclinical results in sheep were encouraging.[10,23] Commercially available SynerGraft valves, however, failed catastrophically in children due to a severe inflammatory reaction.[24] Subsequent identification of whole cells, DNA, and the α-Gal epitope in the walls of SynerGraft

[1]Faculty of Biological Sciences, School of Biomedical Sciences, University of Leeds, Leeds, United Kingdom.
[2]Yorkshire Heart Centre, Leeds General Infirmary, Leeds, United Kingdom.
[3]Institute of Medical and Biological Engineering, School of Mechanical Engineering, University of Leeds, United Kingdom.
[4]Department of Cardiac Surgery, Santa Casa de Curitiba, Pontifica Universidade Catolica do Parana, Curitiba, Parana, Brazil.
[5]NHS Blood & Transplant Tissue Services, Estuary Bank, Speke, Liverpool, United Kingdom.

© J.R. Paniagua Gutierrez *et al.* 2015; Published by Mary Ann Liebert, Inc. This Open Access article is distributed under the terms of the Creative Commons License Attribution-Non-Commercial Share Alike (http://creativecommons.org/licenses/by-nc-sa/4.0/).

porcine valves indicated incomplete decellularization as the likely cause.[25] AutoTissue GmbH later commercialized acellular porcine pulmonary valves; Matrix P® (2004) and Matrix PPlus® (2005) produced using a proprietary process based on 1% sodium deoxycholate. Again, laboratory studies, preclinical studies in sheep, and early clinical studies showed considerable promise.[26–28] Later reports on the performance of these valves were, however, variable.[29–31] Cicha *et al.*[32] reported on four adolescent patients implanted with Matrix P valves, who were reoperated due to early to midterm graft failure (12–15 months). The explanted valves showed massive inflammatory and fibrotic responses at the distal region, lumen narrowing, and low recolonization of the decellularized matrix. Analyses of preimplant control valves revealed incomplete decellularization.

The evidence indicates that incomplete decellularization of porcine valves is associated with graft failure. Considerable caution will be needed before the introduction of porcine valves decellularized using alternative processes in the future. We have developed processes for the decellularization of porcine aortic roots, which have shown effective cell removal, excellent biocompatibility, and preservation of biomechanical function.[33–36] In this study, we report on early preclinical studies of the low-concentration SDS-decellularized porcine aortic valves in the descending aorta of pigs and the right ventricular outflow tract (RVOT) of sheep. The studies revealed an intriguing involvement of macrophages in the remodeling of the acellular tissue.

Materials and Methods

Porcine aortic roots

Aortic roots were harvested from 7 kg (9 mm diameter) and 25 kg (15 mm diameter), large, white female pigs sourced from the UK Home Office Approved farms. Following humane killing, hearts were aseptically harvested and placed into sterile phosphate-buffered saline (PBS; ICN Biomedical) plus 10 $KIU.mL^{-1}$ aprotinin (Bayer), 100 $U.mL^{-1}$ penicillin (Invitrogen), and 100 $\mu g.mL^{-1}$ streptomycin (Invitrogen). Aortic roots were dissected, trimmed of excess tissue, rinsed in supplemented PBS, and stored dry on moist filter paper at −40°C.

Ovine aortic roots

Eight 25 kg Suffolk sheep were sourced from ''Fazenda Experimental Gralha Azul PUCPR,'' Brazil. The sheep were humanely sacrificed and the aortic roots were dissected as above.

Decellularization of porcine aortic roots

This technique has been described previously.[33–35] A total of 16 porcine aortic roots (15 mm diameter) were decellularized. The adventitial and intimal surfaces of the aortic wall were treated with 0.5% (w/v) agarose gel containing 1.25% (w/v) trypsin (type II-S from porcine pancreas, 1800 BAEE $U.mg^{-1}$; Sigma) sparing the leaflets, in a humidified container for 4 h at 37°C. Unless stated otherwise, all subsequent washes were at ambient temperature with agitation. Roots were washed (3 × 30 min) in PBS containing 0.1% (w/v) EDTA (Sigma), 45 $\mu g.mL^{-1}$ trypsin inhibitor (Sigma), and 10 $KIU.mL^{-1}$ aprotinin, before they were immersed in a hypotonic Tris buffer (HTB; 10 mM tris, pH 8.0 containing 0.1% [w/v] EDTA plus 10 $KIU.mL^{-1}$ aprotinin) and incubated for 16 h at 4°C. The roots were washed in PBS plus protease inhibitors and incubated in 0.1% (w/v) sodium dodecyl sulfate (SDS; Calbiochem) in HTB for 24 h before they were washed overnight (~16 h) in PBS containing aprotinin (10 $KIU.mL^{-1}$) and incubated in a nuclease solution (RNase, 1 $U.mL^{-1}$ and DNase 50 $U.mL^{-1}$ in 50 mM Tris-HCl, 10 mM $MgCl_2$, and 50 $mg.mL^{-1}$ bovine serum albumin; pH 7.5; all Sigma) for 4 h at 37°C. The roots were then washed in PBS for 3 days at 37°C, immersed in peracetic acid (0.1% w/v; Sigma) for 3 h before the final washes, and stored in PBS before analysis or cryopreservation. Two roots were processed for histological analysis, six were utilized for biomechanical testing, and eight were cryopreserved for shipping to Brazil for implantation in juvenile sheep.

Three 9-mm-diameter porcine aortic roots were decellularized, as described above, with the exception that trypsin treatment was not used. The roots were dry frozen before implantation in pigs.

Cryopreservation of 15 mm acellular porcine and native ovine aortic roots

Each root was cryopreserved in 100 mL cryopreservation solution (82.5 mL Hanks balanced salt solution with 2.5 mL 1 M HEPES buffer and 15 mL 16% (w/w) dimethyl sulfoxide; Pharmacy Manufacturing Unit; Ipswich NHS Hospital, UK). Frozen porcine roots were shipped on dry ice to the University Veterinary Hospital ''Hospital Veterinário Para Animais De Companhia'' PUCPR São José Dos Pinhais, Brazil, where they were stored at −80°C until implanted.

Biomechanical tests

Root dilation tests were performed as described by Korossis *et al.*[36] The roots were pressurized from 0 to 120 mmHg in 20 mmHg intervals. At each increment, an image of the root was recorded using a video camera. The images were calibrated and analyzed using Image-Pro Plus™ (Media Cybernetics). The dilation of each root at a given pressure was recorded as the external root diameter half way between two reference points. Uniaxial tensile testing to failure was carried out on circumferential and axial aortic wall strips (5 × 20 mm) using a Howden tensile testing machine according to Korossis *et al.*[34] Specimens were preloaded to 0.01 N and loaded to failure using a positive ramp function at 10 $mm.min^{-1}$ at 20°C. Failure was taken at the first decrease in load during extension. Load and extension data were acquired at a rate of 20 Hz and converted to stress–strain. Data acquisition was performed using the MTT.exe software. The stress–strain behavior of the specimens was analyzed by means of the elastin (EI-E)-phase and collagen (Coll-E)-phase moduli, transition stress (σ_T) and strain (ε_T), ultimate tensile strength (σ_{UTS}), and failure strain (ε_{UTS}).

Implantation of acellular allogeneic and fresh allogeneic 9-mm-diameter porcine aortic roots in the abdominal aorta of pigs

Operative procedure. Three fresh and three acellular porcine aortic roots were implanted in 25 kg, large, white female pigs. All procedures were conducted under appropriate UK Home Office Project and Personal Licences. The animals received prophylactic amoxicillin 15 $mg.kg^{-1}$ and were

Table 1. Antibodies, Antigen Retrieval Methods, and Controls Used for Immunohistochemical Analysis

Antibody	*Supplier*	*Dilution*	*Antigen retrieval method*	*Pig explants*		*Sheep explants*	
				Control	*Detection*	*Control*	*Detection*
Von Willebrand factor/factor VIII complex Rabbit anti-human	Dako A0082	1:500	Citrate microwave	Porcine tonsil	IP	MaxArray™ Sheep tissue (Zymed)	Anti-rabbit/mouse envision Dako K 5007
α-Smooth muscle actin Mouse anti-human	Dako M0851 clone A4	1:500	Citrate microwave	Porcine colon	IP	MaxArray Sheep tissue (Zymed)	Anti-rabbit/mouse envision Dako K 5007
CD3 Mouse anti-human	Vision Biosystems NCL-CD3-365	1:50	Heat induced	Porcine spleen	IP	MaxArray Sheep tissue (Zymed)	Anti-rabbit/mouse envision Dako K 5007
Macrophage Mouse anti-human	Serotec MCA874G Clone MAC387	1:50	Trypsin	Porcine spleen	IP	MaxArray Sheep tissue (Zymed)	Anti-rabbit/mouse envision Dako K 5007
Ki67 Mouse anti-human	Dako M7240 Clone MIB-1	1:50	Citrate microwave	Porcine skin	IP	MaxArray Sheep tissue (Zymed)	Anti-rabbit/mouse envision Dako K 5007
Vimentin	Vision Biosystems NCL-L-VIM-V9 Clone V9	1:400	Citrate microwave	Porcine aorta	IP	MaxArray Sheep tissue (Zymed)	Anti-rabbit/mouse envision Dako K 5007

Citric acid buffer consisted of 10 mM citric acid pH 6.0, sections were microwaved on full power for 10 min. Trypsin antigen retrieval was carried out by incubating in 0.1% (w/v) trypsin in 0.1% (w/v) $CaCl_2$ at a pH of 7.8 for 10 min at 37°C. EDTA heat-induced epitope retrieval was carried out in 10 mM Tris buffer 1 mM EDTA, pH 9.0, sections were microwaved on full power for 10 min.

IP, immunoperoxidase.

premedicated, anesthetized, mechanically ventilated, and monitored throughout the procedure.

The abdomen was opened through a midline incision and the infrarenal aorta was exposed. The aorta was clamped and divided without removing any aortic tissue. The valve was anastomosed proximally and distally using a 6/0 non-absorbable, monofilament, and continuous stitch. The aorta was declamped and hemostasis secured. The abdominal wall was then closed in layers. Pigs received a 20 mg subcutaneous dose of a low-molecular-weight heparin (Clexane; Rhône-Poulenc Rorer) for 6 days postoperatively and were sacrificed at 6 weeks (pentobarbital; 20% w/v; 1 $mL.kg^{-1}$). A laparotomy was performed and the aortic root explanted.

Implantation of acellular xenogeneic porcine and native allogeneic ovine 15 mm aortic roots in the RVOT of juvenile sheep

Seven acellular 15 mm porcine aortic roots and seven native ovine aortic roots were implanted in the RVOT of juvenile sheep (3–4 month old; 19–22 kg) at the Hospital Veterinário Para Animais De Companhia PUCPR in accordance with the institutional guidelines for animal care. The study was approved by the Ethics Committee of Researches PUC-PR. The cryopreserved roots were gently thawed at 37°C, washed aseptically in 0.9% (w/v) saline solution, trimmed, and kept moist until implanted.

Operative procedure. The animals received prophylactic gentamicin 4 $mg.kg^{-1}$ and cephalosporin 2 $mg.kg^{-1}$. The operations were performed through a left thoracotomy through the third intercostal space using normothermic cardiopulmonary bypass, as described previously.[26] A segment of the pulmonary artery was resected and the pulmonary valve leaflets were removed. The grafts were interposed in the orthotopic position and anastomosed using 5/0 prolene continuous suture proximally and distally.

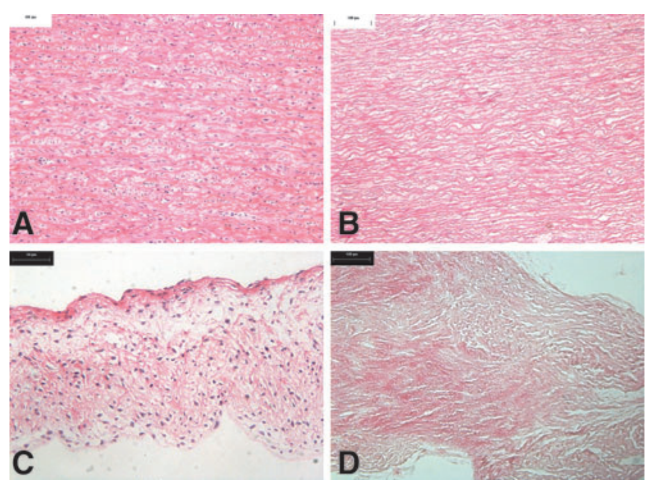

FIG. 1. Histology of native **(A, C)** and decellularized **(B, D)** porcine 15 mm aortic roots. **(A)** Native aortic wall (×100). **(C)** Native aortic valve leaflet (×100). **(B)** Decellularized aortic wall showing an absence of cells (×100). **(D)** Decellularized aortic valve leaflet showing an absence of cells (×100).

Monitoring. All of the animals were weighed at 10, 30, and 60 days. At 6 months, the grafts were retrieved under general anesthesia and the animals were sacrificed (KCl 19.1% iv).

Analysis of explanted roots

All explanted roots were surveyed macroscopically and photographed. The explanted 15 mm aortic roots were cryopreserved and shipped back to the University of Leeds, UK, for analysis. Three explanted decellularized porcine (EDP 1,3,7) and three explanted sheep controls (ES 1,3,7) were dissected longitudinally to obtain blocks for histological and immunohistochemical investigations. The remaining portions of these three roots were used for calcium analysis. Four explanted roots from each group (EDP 2,4,5,6 and ES 2,4,5,6) were utilized for biomechanical testing and calcium analysis.

Histological analysis

Tissue specimens were fixed (10% [v/v] neutral buffered formalin), dehydrated, and embedded in paraffin wax. Ten serial sections of 5 μm were taken longitudinally at six levels, 150 μm apart. One section at each level was stained with hematoxylin and eosin (H&E), Van Gieson, Miller's elastin, and Von Kossa. Sections were dehydrated and mounted in DPX, and images were captured using an Olympus microscope (OL BX51, Olympus) and digital camera (Evolution MP color).

Immunocytochemical analysis

The primary antibodies, dilutions, antigen retrieval methods, and control tissues used are listed in Table 1. Isotype control antibodies and omission of the primary antibodies were used to verify antibody specificity and as negative controls. Immunolabeling using the avidin–biotin complex (ABC) immunoperoxidase system (pig explants) was carried out at room temperature, and Tris-buffered saline (TBS; 50 mM Tris, 150 mM NaCl, pH 7.6) was used as the diluent and wash buffer. Sections were incubated in 3% (v/v) H_2O_2 before antigen retrieval and blocked with avidin–biotin blocking reagents (Vector Labs) and 20% (v/v) rabbit serum (Vector Labs). Sections were incubated with 50 μL of primary antibody for 1 h (overnight at 4°C for MAC 387), 50 μL of secondary antibody (biotinylated rabbit anti-mouse Ig F[ab']2 fragments; Dako) for 30 min, and 50 μL of horseradish peroxidase streptavidin (Vector Labs) for 30 min with three washes between each step. The bound antibody was visualized using Sigma Fast 3,3′-diaminobenzidine (DAB). Sections were counterstained in hematoxylin, dehydrated, and mounted in DPX (VWR).

Immunolabeling with the Dako EnVision System-HRP (sheep explants) involved blocking the sections with peroxidase block (Dako), incubation with the primary antibody for 30 min, and incubation in peroxidase labeled polymer (Envision solution; DAKO EnVision™ +System, HRP). The bound antibody was visualized by incubation in DAB for 5–10 min, and sections were counterstained, dehydrated, and mounted as above.

Quantitative calcium analysis by inductively coupled plasma—mass spectrometry (ICPMS)

Tissue samples ($n = 3$–7; 2–4 mm^2) were freeze-dried to constant weight, digested in 0.25 mL of nitric acid and

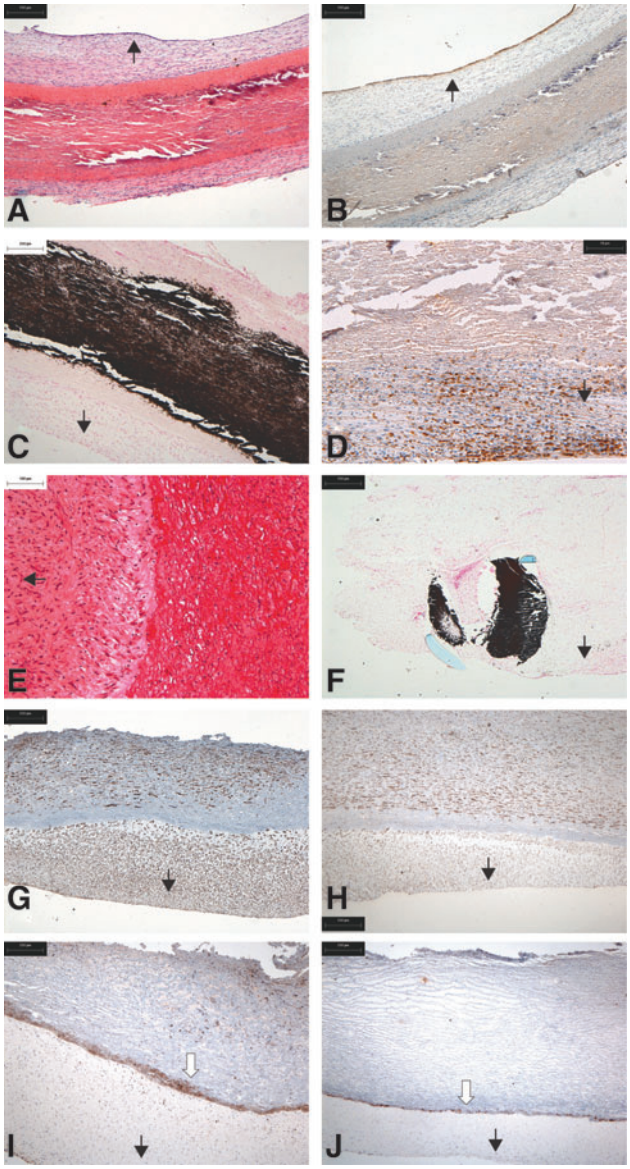

FIG. 2. Histological and immunohistochemical findings in explanted native **(A–D)** and decellularized **(E–J)** porcine 9-mm-diameter aortic roots following 6 weeks of implantation in the descending abdominal aorta of pigs. **(A)** H&E-stained section of native explant showing the formation of a neointima and adventitia with destruction of the implanted tissue (×40). **(B)** Immunostaining for von Willebrand factor showing the formation of a continuous endothelium (×40). **(C)** Von Kossa-stained section showing extensive calcification of the implanted native tissue (×40). **(D)** Immunostaining for CD3 indicating the presence of T cells around the native tissue (×100). **(E)** H&E-stained section of decellularized explant showing the presence of cells within the tissue (×100). **(F)** Von Kossa-stained section of the suture point (×100). **(G)** Immunostaining for α-smooth muscle actin (α-SMA) indicating that the majority of cells are smooth muscle cells (×40). **(H)** Immunostaining for vimentin showing the extensive presence of aligned cells in the implanted tissue (×40). **(I, J)** Immunostaining for MAC clearly showing a wall of macrophages at the interface between the neointima and the implanted tissue from both explants highlighted by the *white arrow* (×40). *Black arrows* indicate the direction of aortic lumen. H&E, hematoxylin and eosin.

0.25 mL of hydrogen peroxide (both Romil-SpA, Super Purity Acids & Reagents), and heated to 90°C for 2 h. Calcium analyses were performed on an Elan 6100 ICP-MS (Perkin-Elmer SCIEX) calibrated using Ca ICPMS ARISTAR single element standard (Merck BDH).

Data analysis

Quantitative data are expressed as the mean ± 95% confidence interval. The data were analyzed by one-way analysis of variance (ANOVA) followed by calculation of the minimum significant difference (MSD; $p < 0.05$) between group means using the T method.

Results

Histology of decellularized porcine aortic roots

Representative images of H&E-stained sections of the native and decellularized 15 mm roots are shown in Figure 1 and showed no evidence of cells or cell remnants in the acellular tissues.

In vivo *assessment of decellularized porcine aortic roots in the descending aorta of pigs*

One pig from the acellular group developed signs of abdominal discomfort 2 days postoperatively and was humanely killed. A postmortem examination revealed a small bowel obstruction. A gross examination of the acellular and native control roots explanted at 6 weeks revealed major differences. The explanted acellular roots had lost their leaflets and their walls were soft and pliable with no overt signs of calcifications, thrombi, or vegetations. The explanted native porcine roots had retracted thickened leaflets and their walls were overtly calcified and hard.

A neointima had formed on the luminal surface of native control tissues (Fig. 2A) with a confluent layer of endothelial cells (Fig. 2B). The medial layer of the native control tissues was severely damaged (Fig. 2A, B) and heavily calcified (Fig. 2C). The calcified areas were heavily infiltrated by $CD3^+$ T cells (Fig. 2D). There were few MAC-positive cells, indicating a paucity of macrophages. The cells in the neointima and adventia were vimentin positive. The cells in the neointima and blood vessels in the adventia were α-smooth muscle actin (α-SMA) positive.

H&E-stained sections of the explanted acellular roots revealed a demarcation between the implanted tissue and neointima (Fig. 2E). The medial layer showed no evidence of damage and calcification except at the suture points (Fig. 2F). Interstitial cells positive for α-SMA and vimentin were present in the media (Fig. 2G, H). There was no evidence of $CD3^+$ T cells in the acellular explants, with the exception of a few $CD3^+$ cells at the suture points. The most striking observation for the acellular root tissue was the presence of macrophages (MAC-positive cells) in a strongly demarcated line below the neointima of the explanted tissue from both implants (Fig. 2I, J).

In vivo *assessment of decellularized porcine aortic roots in the RVOT of juvenile sheep*

The animals were weighed at 0, 10, 30, and 60 days and steadily increased in weight over the period. Roots were explanted at 6 months.

The explanted seven sheep aortic control roots were all (explanted sheep; ES1-7) hard, rigid, and heavily calcified at explantation. The root walls and leaflets were retracted. Five of the explanted decellularized porcine roots (explanted decellularized porcine; EDP1 and 4–7) were soft with no evidence of thrombus, vegetation, pannus, or stenosis. The leaflets were undamaged, and calcification was only evident at the suture points. EDP2 and EDP3 had no thrombus or vegetation, however, there was some pannus formation and stenosis and they were rubbery/firm to touch. The leaflets of these two explants were thickened and retracted. Example macroscopic images are shown in Figures 3.

Histology of explanted ovine roots ES1, 3, and 7 showed extensive damage. The damaged walls had a thickened neointima and a developed adventitia. The leaflets were retracted and thickened (Fig. 4A, B). The tissues were

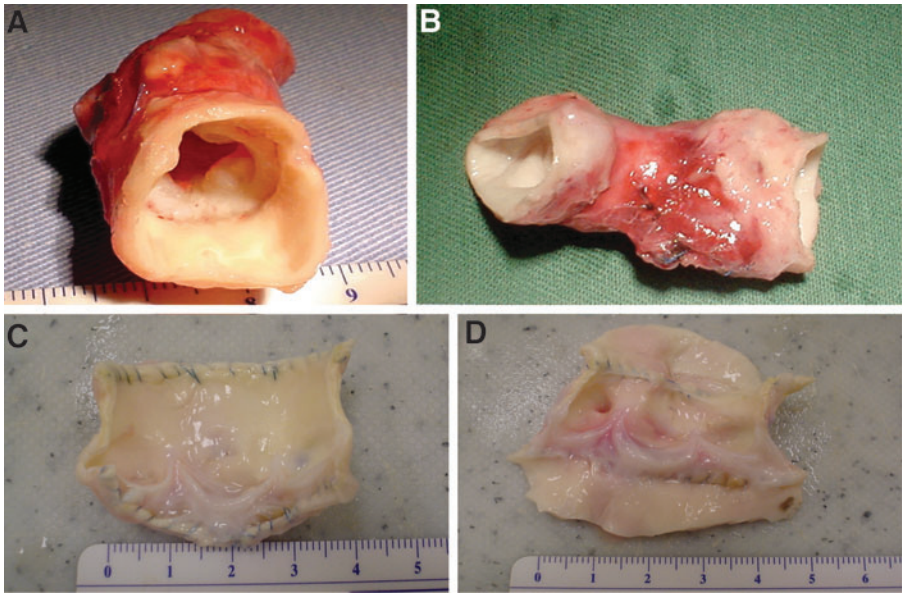

FIG. 3. Macroscopic appearance of explanted aortic roots following 6 months implantation in the right ventricular outflow tract of juvenile sheep. **(A)** Explanted acellular porcine aortic root EDP2 showing some retraction of the leaflets inside the rubbery wall. **(B)** Explanted native ovine root ES2 showing the rigid tube-like appearance of the retracted root within the pulmonary wall. **(C** and **D)** Explanted acellular porcine roots EDP4 and EDP5 opened up to show leaflets. These valves were soft to the touch with no gross evidence of leaflet damage or stenosis.

heavily calcified (Fig. 4C, D). $CD3^+$ cells were present around the damaged areas of the wall (Fig. 4E, F) and in the leaflets. The $CD3^+$ cells were of a proliferative phenotype, as revealed by Ki-67 labeling (Fig. 4G). There was a notable paucity of macrophages associated with the immunological rejection response (Fig. 4H).

An overview of the histology of the explanted decellularized porcine roots EDP 1, 3, and 7 is presented in Figure 5. Roots EDP1 and EDPD7 were integrated with remodeling of the acellular tissue, with formation of a neointima and well-formed adventitia. Minimal calcification was observed, limited to the suture points (Fig. 5D, F). Root EDP3 also showed integration and remodeling, however, there was a line of calcification in the central region of the aortic wall (Fig. 5E).

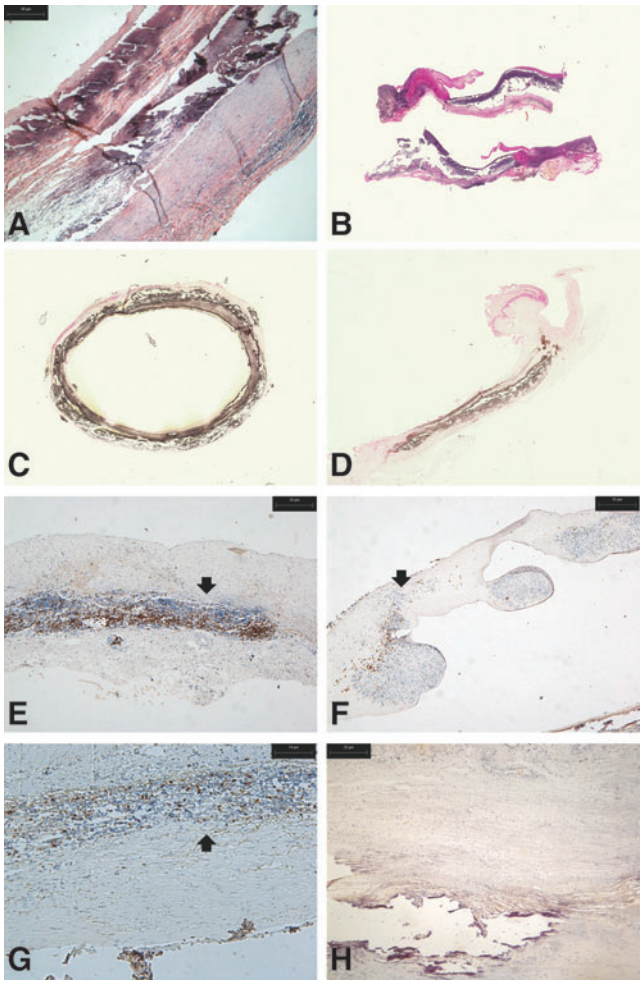

FIG. 4. Histological and immunohistochemical findings in explanted native ovine 15-mm-diameter aortic roots following 6 months implantation in the right ventricular outflow tract of juvenile sheep. **(A)** H&E-stained section of explanted root ES3 showing extensive damage to the root wall (×40). **(B)** Elastin van Gieson-stained longitudinal sections of aortic roots ES3 (*upper*) and ES7 (*lower*) showing that the damage to the wall extended the lengths of the implants and showing the thickened retracted leaflets (×4). **(C)** Von Kossa-stained cross-sectional view of aortic root ES1 showing that calcification was present throughout (×4). **(D)** Von Kossa-stained longitudinal section of aortic root ES3 showing calcification of the wall (×4). **(E)** Immunostaining for CD3 in aortic root wall of ES3 showing T-cell infiltrate (*arrow*) (×40). **(F)** Immunostaining for CD3 in leaflet of root ES3 showing T-cell infiltrate (*arrow*) (×40). **(G)** Immunostaining for Ki-67 in aortic root wall of ES3 showing the presence of proliferative cells (*arrow*) (×40). **(H)** Immunostaining for MAC in aortic root wall of ES1 showing the absence of macrophages (×40).

There was a central acellular wall area in these explants surrounded by a cellular area (Fig. 6A), highlighted by immunostaining for vimentin (Fig. 6B). The leaflets of the decellularized aortic roots retained their trilaminar structure. They were recellularized with stromal cells and covered in a layer of Von Willebrand Factor-positive cells (Fig. 6C, D). Immunostaining for α-SMA showed that cells in the medial area of the aortic wall were of the smooth muscle cell phenotype and also highlighted the presence of blood vessels in the adventitia (Fig. 6E). In the leaflets, the cells were largely α-SMA negative with the exception of the cells at the surface (Fig. 6F). As observed in the pig study, the most striking feature was the presence of MAC-positive cells demarking the interface between the acellular portion of the aortic wall and the recellularized areas. This was evident in all three of the explanted aortic roots (Fig. 6G, I, J). Macrophages were not evident in the leaflets of any of the aortic roots nor were $CD3^+$ cells. T cells were only found in EDP3 associated with the calcified area of the aortic wall (Fig. 6H).

Quantitative calcium analysis

The native and decellularized porcine tissue had very low calcium content, as did the explanted decellularized porcine and ovine aortic valve leaflets (Fig. 7). The explanted ovine aortic wall tissue contained 43,485 to 472,728 μg calcium per gram of tissue. The explanted decellularized porcine aortic wall tissue also showed a highly variable calcium content ranging from 925 to 69,191 $\mu g.g^{-1}$.

Biomechanical studies of native, decellularized, and explanted aortic roots

There was no significant difference in the dilation of the fresh and decellularized roots up to 120 mmHg. There was also no difference in the mechanical properties of the preimplant native and decellularized aortic wall tissue (Table 2). However, there was a small but significant reduction in the thickness of the tissue following decellularization ($p < 0.05$).

For the explanted decellularized porcine compared to the preimplant aortic wall tissue, there was no significant difference in the thickness, elastin phase modulus, or collagen phase modulus in the axial or circumferential directions (Table 2). In the axial direction, there was no significant difference in the transition stress or the ultimate tensile stress. In the circumferential direction, the transition stress and ultimate tensile stress were reduced ($p < 0.05$). The transition and failure strains were reduced in both directions, indicating a less extensible or permanently extended tissue (Table 2).

For the explanted native ovine valves, there was no preimplant sheep valve data for comparison. The properties were compared to the native and decellularized porcine tissue, although it is recognized that this is not a direct comparison. The elastin phase modulus was higher in the circumferential

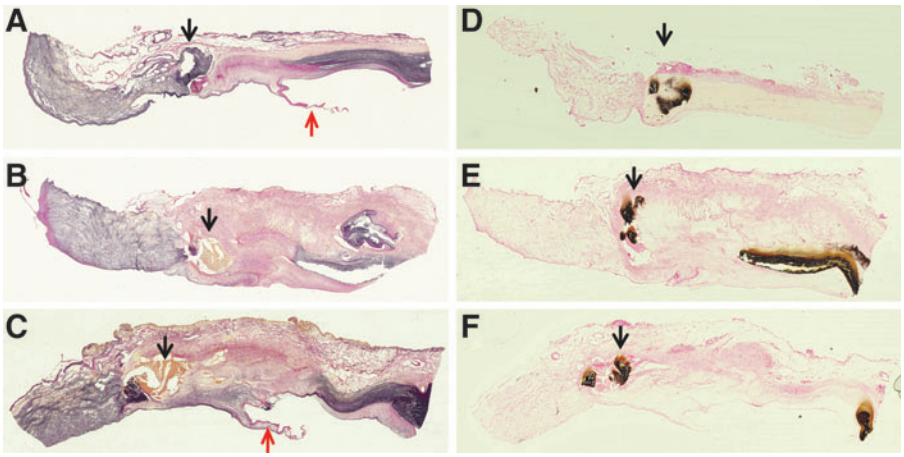

FIG. 5. Low-power overviews of the histology of explanted decellularized porcine 15-mm-diameter aortic roots following 6 months implantation in the right ventricular outflow tract of juvenile sheep. **(A–C)** Elastin van Gieson-stained longitudinal sections of aortic roots EDP1, EDP3, and EDP7, respectively, showing integration and remodeling of the aortic walls and thin leaflets. **(D–F)** Von Kossa-stained longitudinal sections of aortic roots EDP1, EDP3, and EDP7, respectively, showing the location of calcium deposits at the suture points of all roots and evidence of some calcification in the central region of the wall of aortic root EDP3. *Black arrows* indicate suture points and *red arrows* indicate leaflets.

direction and the collagen phase modulus was higher in the axial direction ($p<0.05$), indicating a stiffer tissue. The transition stress and ultimate tensile stress were lower in the circumferential direction ($p<0.05$). The transition and ultimate failure strains were also lower ($p<0.05$) in the explanted ovine wall tissue in both directions, indicating a less extensible or permanently extended tissue.

Discussion

The aims of this study were to determine the functional biocompatibility of low-concentration SDS-decellularized porcine aortic roots *in vivo*. A previously developed process[33–36] was modified for 9- and 15-mm-diameter aortic roots to facilitate implantation into growing animals. Limited evaluation of the decellularized tissue showed a lack of cells, and biomechanical tests (15 mm roots) showed that the decellularized roots were not significantly affected by the process.

Acellular roots (9 mm) were initially implanted into the descending aorta of pigs in a limited study to assess biocompatibility in the hemodynamic environment. Upon explantation at 6 weeks, the acellular roots were not calcified, but had lost their leaflets, most likely due to the more continuous blood flow in the abdominal aorta, which would have kept the leaflets permanently open, causing resorption. In contrast, the explanted native control roots were overtly calcified and the leaflets were present, although retracted. Early calcification of the native allografts may have maintained the rigidity of the leaflets. Although this model had limitations, it revealed some interesting findings. The acellular root walls had largely been regenerated with cells, with a neointima and a luminal surface with a layer of von Willebrand factor-positive cells. There was no calcification of the decellularized roots or the presence of T cells. This was in marked contrast to the native allograft roots, which were overtly calcified, infiltrated with T cells, and severely disrupted, demonstrating the intensity of the immune response to the cellular allografts.

Of particular interest was the presence and pattern of distribution of macrophages in the explanted acellular roots. High-intensity staining for MAC-positive cells was found in a well-demarcated line between the implant and the neointima. Recent knowledge of the plasticity of macrophages favors the idea that the host macrophage response is an essential component of the acellular biological scaffold remodeling process.[37,38] The presence of macrophages at the boundary of the implanted root wall tissue with concomitant stromal cell infiltration in the absence of T cells, tissue damage, and fibrosis was highly suggestive that the acellular tissue was undergoing a remodeling process, orchestrated by the macrophages.

It is now recognized that macrophages may adopt heterogeneous phenotypes forming a spectrum from proinflammatory classically activated macrophages (often referred to as M1) to anti-inflammatory, wound healing inflammation-resolving phenotypes involved in homeostasis (referred to as M2[37–39]). Studies conducted by the Badylak group have characterized the macrophage response to a range of acellular extracellular matrix scaffolds (reviewed in Brown *et al.*[37]), and they have suggested that a macrophage response is an essential component of the remodeling process of biological extracellular matrix scaffolds.[38] It is interesting to note that work published after the completion of the present study on the performance of acellular porcine aortic valves in the RVOT of pigs also demonstrated self-regeneration potential after 15 months and that macrophages with a reparative M2 phenotype were present in high numbers in the repopulated valves.[40]

The sheep is the most widely used model for evaluation of cardiac valves[10,23,26,27] and as an accelerated calcification model most closely modeling human physiology. The acellular porcine roots were implanted into the RVOT to avoid undue suffering of the animals in the event of failure. It should be noted that there were two major differences in the preparation of the acellular porcine aortic roots for the studies in sheep compared to the studies in the pig model.

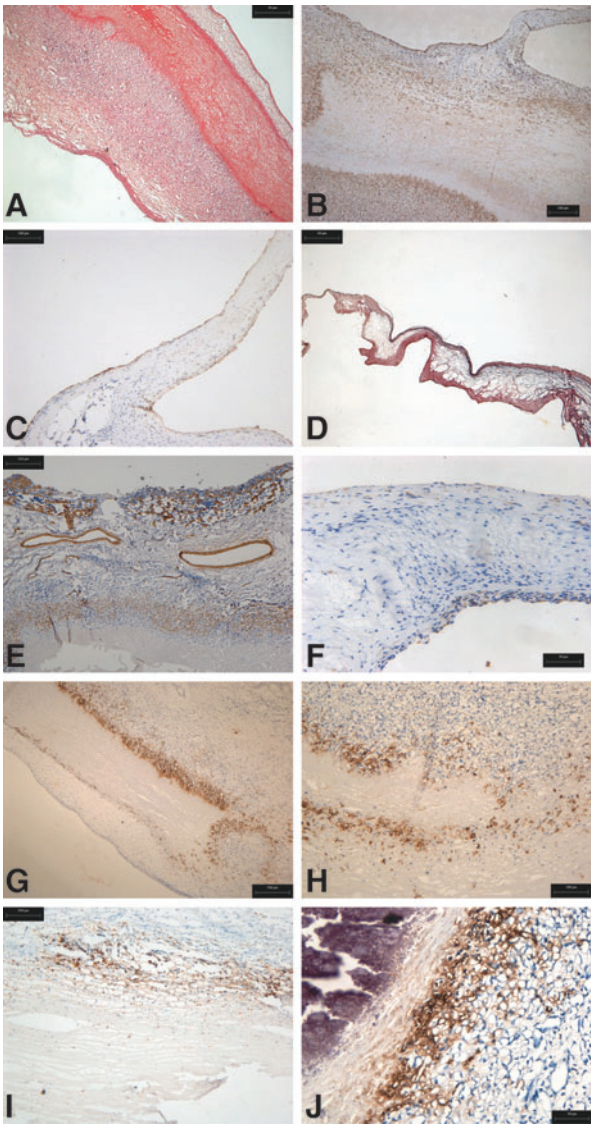

FIG. 6. Histological and immunohistochemical findings in explanted decellularized porcine 15-mm-diameter aortic roots following 6 months implantation in the right ventricular outflow tract of juvenile sheep. **(A)** H&E-stained section of the wall of aortic root EDP1 showing the presence of a neointima and area of root without cells present and area of root that had recellularized (×40). **(B)** Wall from aortic root EDP1 immunostained for vimentin clearly showing the extent of recellularization of the implanted tissue (×40). **(C)** Aortic root EDP1 immunostained for Factor VIII showing the endothelialization of the leaflets (×40). **(D)** Aortic root EDP7 stained by Van Gieson (×40). **(E)** Aortic root EDP7 immunostained for α-SMA showing the vascularized adventitia and smooth muscle cells in the aortic wall (×40). **(F)** Aortic root EDP1 immunostained for α-SMA showing that the majority of cells in the leaflet were negative for this smooth muscle cell marker (×100). **(G)** Aortic root EDP1 and **(H)** aortic root EDP7 showing a clear wall of macrophages demarking the interface between the acellular and cellularized tissues (×40). **(I)** Aortic root EDP3 taken in from the calcified wall area immunostained for CD3 showing the presence of T cells (×40). **(J)** Aortic root EDP3 taken from the calcified wall area immunostained for MAC again showing a clear wall of macrophages demarking the interface between the acellular and cellularized tissues (×100).

The larger 15 mm acellular aortic roots were treated with trypsin (to the outer portion of the aortic wall) and cryopreserved before implantation. Upon explantation of the acellular porcine roots, it was evident that two (EDP2 and EDP3) of the seven roots had undergone mild calcification. Explanted acellular porcine roots (EDP1, EDP3, and EDP7) showed regeneration. The leaflets of all three valves were devoid of calcification and were endothelialized. The matrix of the leaflets retained the characteristic trilaminar structure and was populated by α-SMA-negative and vimentin-positive cells, indicating a fibroblastic and not myofibroblastic phenotype. Similar repopulation of decellularized porcine pulmonary valve leaflets in sheep has been reported previously.[26–28]

The wall of the three acellular explants revealed incomplete recellularization. A neointima had formed on the luminal surface and there was a well-established vasa vasorum. Approximately two-thirds of the wall of all three acellular explants was populated by smooth muscle cells. Interestingly, there was a line of macrophages demarking the nonrepopulated portion in all three acellular explants, again suggesting that the macrophages were orchestrating the repopulation of the acellular tissue as had been observed in the pigs. This feature of the regeneration of acellular porcine cardiac valves in the sheep has not been reported previously, although Erdbrugger *et al.* noted the presence of some monocytes in the explanted decellularized pulmonary root wall.[28] Of note, Leyh *et al.*[41] used immunohistochemical staining for CD11b (Mac-1) in their study of trypsin/EDTA decellularized porcine pulmonary valve repopulation in sheep and found no evidence of positive cells. These differences could be due to a different host response to tissues decellularized using different processes.

There were no T cells present in explanted roots, EDP1 and EDP7. However, a mild infiltrate of $CD3^+$ T cells was associated with a band of calcification in the central portion of the wall of root EDP3. The explanted native allogeneic roots showed extensive calcification of the root walls and a predominant role of T cells in the allogeneic rejection response. Quantitative calcium analysis of all the explanted root tissues supported the histological findings. It is difficult to interpret the calcium data for the decellularized root wall explants since Von Kossa staining revealed calcification at the suture points. Chronic inflammation[42] and calcification[43] in response to polypropylene sutures in blood vessel walls have been reported previously. Given the gross observation of explanted root EDP2, it was likely that this also had some calcification in the wall. The presence of areas of calcification in the explanted decellularized root tissue also makes interpretation of the biomechanical data difficult. The finding of less extensible tissue following implantation would be in keeping with some degree of calcification of the tissue *in situ*. Since both axial and circumferential tissue strips were cut from the explanted root wall distal to the leaflets, they would not have avoided the calcification around the suture points. No previous studies of decellularized porcine cardiac valves in sheep have investigated the biomechanical properties of the tissues.[10,23,26–28,41]

Overall, these studies demonstrated the regenerative potential of low-concentration SDS-decellularized aortic roots in the sheep model and also revealed that the decellularization process was not complete for all of the

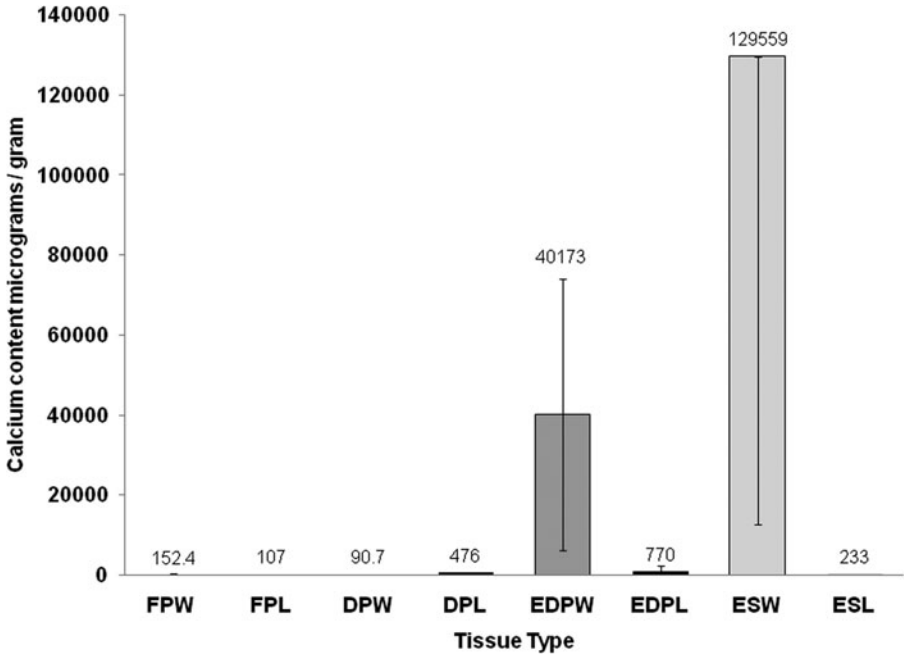

FIG. 7. Calcium content of tissues. Data are presented as means ± 95% confidence limits. Data were analyzed by ANOVA followed by calculation of the MSD ($p < 0.05$) using the T method. This revealed significantly higher levels of calcium in the explanted ovine aortic wall tissue compared to all other groups except the explanted acellular porcine aortic wall tissue. FPW, fresh porcine aortic wall ($n = 8$); FPL, fresh porcine leaflet ($n = 8$); DPW, decellularized porcine aortic wall ($n = 6$); DPL, decellularized porcine leaflet ($n = 6$); EDPW, explanted porcine aortic wall ($n = 6$); EDPL, explanted porcine leaflet ($n = 3$); ESW, explanted sheep aortic wall ($n = 7$); ESL, explanted sheep leaflet ($n = 7$).

implanted roots. Additionally, three 15 mm porcine aortic roots were therefore decellularized and analyzed for evidence of residual cells. A close examination of the H&E-stained sections (Fig. 8) revealed residual nuclear material in the central portion of the tissue, confirming incomplete decellularization. It was noteworthy that the area of incomplete decellularization was in the same area of the root wall that was calcified in the explanted decellularized root EDP3, indicating that calcification was most likely associated with residual DNA in the tissue and highlighting the role of DNA as a *nidus* for calcification. Subsequent studies have focused upon reoptimization of the decellularization process.

Despite obvious limitations, the studies have highlighted (1) the importance of complete decellularization of porcine cardiac valved roots to avoid calcification and (2) the need for further studies of the phenotype of macrophages responding to decellularized porcine cardiac root tissues in large animal models with a view to determining whether they are of the proinflammatory phenotype or express markers indicative of anti-inflammatory, wound healing, inflammation resolving, or fibrolytic phenotypes.

Table 2. Biomechanical Analysis of the Fresh, Decellularized, and Explanted Aortic Wall Tissue

	EI-E(MPa)	*Coll-E (MPa)*	σ_T *(MPa)*	ε_T *(%)*	σ_{UTS} *(MPa)*	ε_{UTS} *(%)*	*Thickness (mm)*
Axial							
FP	0.11 ± 0.02	1.83 ± 0.70	0.19 ± 0.08	62.7 ± 11.43	0.74 ± 0.30	108.2 ± 13.8	1.73 ± 0.32
DP	0.10 ± 0.04	2.04 ± 1.42	0.18 ± 0.11	62.2 ± 13.8	0.70 ± 0.35	127.9 ± 14.1	1.29 ± 0.27
EDP	0.13 ± 0.07	1.53 ± 0.49	0.05 ± 0.02	21.0 ± 10.6 $p < 0.05$ vs. FP,DP	0.49 ± 0.09	55.8 ± 7.2 $p < 0.05$ vs. FP,DP	2.0 ± 1.14
ES	0.28 ± 0.24	4.3 ± 2.19 $p < 0.05$ vs. FP, EDP	0.10 ± 0.04	20.00 ± 6.63 $p < 0.05$ vs. FP,DP	0.87 ± 0.42	47.20 ± 12.9 $p < 0.05$ vs. FP,DP	1.50 ± 0.34
Circumferential							
FP	0.15 ± 0.03	4.95 ± 0.78	0.44 ± 0.01	72.1 ± 8.47	1.96 ± 0.12	112.6 ± 16.9	2.02 ± 0.1
DP	0.11 ± 0.06	4.18 ± 1.84	0.45 ± 0.22	65.9 ± 13.3	1.85 ± 0.86	112.5 ± 20	1.46 ± 0.13 $p < 0.05$ vs. F
EDP	0.12 ± 0.08	4.13 ± 3.57	0.10 ± 0.06 $p < 0.05$ vs. F, DP	23.7 ± 12.25 $p < 0.05$ vs. F, DP	0.72 ± 0.15 $p < 0.05$ vs. F, DP	49.9 ± 21.4 $p < 0.05$ vs. F, DP	1.69 ± 0.11
ES	0.40 ± 0.20 $p < 0.05$ vs. DP	3.42 ± 0.93	0.08 ± 0.03 $p < 0.05$ vs. F, DP	14.0 ± 4.66 $p < 0.05$ vs. F, DP	0.75 ± 0.22 $p < 0.05$ vs. F, DP	39.90 ± 7.0 $p < 0.05$ vs. F, DP	1.72 ± 0.34

Uniaxial tensile tests of the aortic wall tissue ($n = 4$–6) were carried out in the axial and circumferential directions. Data were analyzed by ANOVA followed by calculation of the MSD between group means ($p < 0.05$) using the T method.

FP, fresh porcine; DP, decellularized porcine; EDP, explanted decellularized porcine; ES, explanted sheep; EI-E, elastin phase slope; Coll-E, collagen phase slope; σ_T, transition stress; ε_T, transition strain; σ_{UTS}, ultimate tensile strength; ε_{UTS}, failure strain.

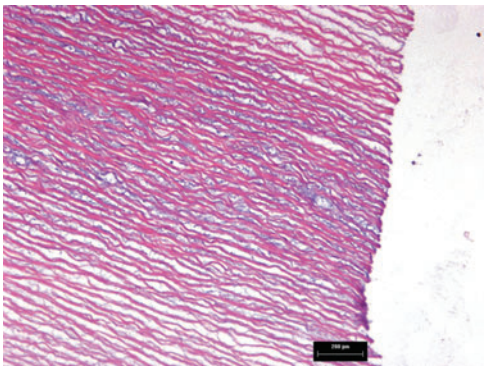

FIG. 8. Hematoxylin and eosin-stained section of decellularized porcine aortic wall tissue. The image reveals evidence of residual DNA in the central region of the tissue, taken from the region next to the commissures (×100).

Acknowledgments

This study was funded by the Children's Heart Surgery Fund, EPSRC, and through WELMEC, a Centre of Excellence in Medical Engineering funded by the Wellcome Trust and EPSRC, under grant number WT 088908/Z/09/Z.

Disclosure Statement

E.I. and J.F. are consultants and shareholders in Tissue Regenix Group plc. SK is a shareholder in Tissue Regenix Group plc. Helen Berry–nee Wilcox is now an employee of Tissue Regenix Group plc.

References

1. Senthilnathan, V., Treasure, T., Grunkemeier, G., and Starr, A. Heart valves: which is the best choice? Cardiovasc Surg **7,** 393, 1999.
2. Gao, G., Wu, Y., Grunkemeier, G.L., Furnary, A.P., and Starr, A. Durability of pericardial versus porcine aortic valves. J Am Coll Cardiol **44,** 384, 2004.
3. O'Brien, M.F., Harrocks, S., Stafford, E.G., Gardner, M.A., Pohlner, P.G., and Tesar, P.J. The homograft aortic valve: a 29-year, 99.3% follow up of 1,022 valve replacements. J Heart Valve Dis **10,** 334, 2001.
4. Dignan, R., O'Brien, M., Hogan, P., Thornton, A., Fowler, K., Byrne, D., Stephens, F., and Harrocks, S. Aortic valve allograft structural deterioration is associated with a subset of antibodies to human leukocyte antigens. J Heart Valve Dis **12,** 382, 2003.
5. Baskett, R.J., Nanton, M.A., Warren, A.E., and Ross, D.B. Human leucocyte antigen-DR and ABO mismatch are associated with accelerated homograft failure in children: implications for therapeutic interventions. J Thorac Cardiovasc Surg **126,** 232, 2003.
6. Ryan, W.H., Herbert, M.A., Dewey, T.M., Agarwal, S., Ryan, A.L., Prince, S.L., and Mack, M.J. The occurence of postoperative pulmonary homograft stenosis in adult patients undergoing the Ross procedure. J Heart Valve Dis **15,** 108, 2006.
7. Carr-White, G.S., Kilner, P.J., Hon, J.K.F., Rutledge, T., Edwards, S., Burman, E.D., Pennel, D.J., and Yacoub, M.H. Incidence, location, pathology and significance of pulmonary homograft stenosis after the Ross operation. Circulation **104 Suppl 1,** 16—20, 2001.
8. Hogan, P.G., and O'Brien, M.F. Improving the allograft valve: does the immune response matter? J Thorac Cardiovasc Surg **126,** 1251, 2003.
9. Elkins, R.C., Lane, M.M., Cappa, S.B., McCue, C., and Dawson, P.E. Humoral immune responds to allograft valve tissue pretreated with an antigen reduction process. Semin Thorac Cardiovasc Surg **13,** 82, 2001.
10. O'Brien, M.F., Goldstein, S., Walsh, S., Black, K.S., Elkins, R., and Clarke, D. The SynerGraft valve: a new acellular (non-gluteraldehyde-fixed) tissue heart valve for autologous recellularisation; first experimental studies before clinical implantation. Semin Thorac Cardiovasc Surg **11 Suppl 1,** 194, 1999.
11. Elkins, R.C., Dawson, P.E., Goldstein, S., Walsh, S.P., and Black, K.S. Decellularised human valve allografts. Ann Thorac Surg **71,** S428, 2001.
12. Hawkins, J.A., Hillman, N.D., Lambert, L.M., Jones, J., Di Russo, G.B., Profaizer, T., Fuller, T.C., Minich, L.L., Williams, R.V., and Shaddy, R.E. Immunogenicity of decellularized cryopreserved allografts in pediatric cardiac surgery: comparison with standard cryopreserved allografts. J Thorac Cardiovasc Surg **126,** 247, 2003.
13. Bechtel, J.F., Gellissen, J., Erasmi, A.W., Petersen, M., Hiob, A., Stierle, U., and Sievers, H.H. Mid-term findings on echocardiography and computed tomography after RVOT-reconstruction: comparison of decellularized (SynerGraft) and conventional allografts. Eur J Cardiothorac Surg **27,** 410, 2005.
14. Tavakkol, Z., Gelehrter, S., Goldberg, C.S., Bove, E.L., Devaney, E.J., and Ohye, R.G. Superior durability of SynerGraft pulmonary allografts compared with standard cryopreserved allografts. Ann Thorac Surg **80,** 1610, 2005.
15. Brown, J.W., Elkins, R.C., Clarke, R.C., Tweddell, J.S., Huddleston, C.B., Doty, J.R., Fehrenbacher, J.W., and Takkenberg, J.J.M. Performance of the CryoValveSG human decellularised pulmonary valve in 342 patients relative to conventional CryoValve at a mean follow-up of four years. J Thorac Cardiovasc Surg **139,** 339, 2010.
16. Burch, P.T., Aditya, K.K., Lambert, L.M., Houbkov, R., Shaddy, R.E., and Hawkins, J.A. Clinical performance of decellularised cryopreserved valved allografts compared with standard allografts in the right ventricular outflow tract. Ann Thorac Surg **90,** 1301, 2010.
17. Ruzmetov, M., Shah, J.J., Geiss, D.M., and Fortuna, R.S. Decellularised versus standard valve allografts for right ventricular outflow tract reconstruction: A single institution comparison. J Thorac Cardiovasc Surg **143,** 543, 2012.
18. Zehr, K.J., Yagubyan, M., Connolly, H.M., Nelson, S.M., and Schaff, H.V. Aortic root replacement with a novel decellularized cryopreserved aortic homograft: postoperative immunoreactivity and early results. J Thorac Cardiovasc Surg **130,** 1010, 2005.
19. Cebotari, S., Tudorache, I., Ciubotaru, A., Boethig, D., Sarikouch, S., Goerler, A., Lichtenberg, A., Cheptanaru, E., Barnaciuc, S., Cazacu, A., Maliga, O., Repin, O., Maniuc, L., Breymann, T., and Haverich, A. Use of fresh decellularised allografts for pulmonary valve replacement may reduce the reoperation rate in children and young adults: early report. Circulation **124,** S115, 2011.
20. daCosta, F.D.A., Dohmen, P.M., Duarte, D., von Glenn, C., Lopes, S.V., Filho, H.H., da Costa, M.B.A., and Konertz, W. Immunological and echocardiographic evaluation of decellularised versus cryopreserved allografts during the Ross operation. Eur J Cardiothorac Surg **27,** 572, 2005.
21. daCosta, F.D., Santos, L.R., Collatusso, C., Matsuda, C.N., Lopes, S.A., Cauduro, S., Roderjan, J.G., and Ingham, E. Thirteen years experience with the Ross operation. J Heart Valve Dis **18,** 84, 2009.

22. da Costa, F.D.A., Costa, A.C.B.A., Prestes, R., Domanski, A.C., Balbi, E.M., Ferreira, A.D.A., and Lopes, S.V. The early and midterm function of decellularised aortic valve allografts. Ann Thorac Surg **90,** 1854, 2010.
23. Goldstein, S., Clarke, D.R., Walsh, S.P., Black, K.S., and O'Brien, M.F. Transpecies heart valve transplant: advanced studies of a bio-engineered xeno-autograft. Ann Thorac Surg **70,** 1962, 2000.
24. Simon, P., Kasimir, M.T., Seebacher, G., Weigel, G., Ullrich, R., Salzer-Muhar, U., Rieder, E., and Wolner, E. Early failure of the tissue engineered porcine heart valve SYNERGRAFT™ in pediatric patients. Eur J Cardiothorac Surg **23,** 1002, 2003.
25. Kasimir, M.T., Rieder, E., Seebacher, G., Wolner, E., Weigel, G., and Simon, P. Presence and elimination of the xenoantigen Gal (a1,3) Gal in tissue engineered heart valves. Tissue Eng **11,** 1274, 2005.
26. dCosta, F.D.A., Dohmen, P.M., Lopes, S.V., Lacerda, G., Pohl, F., Vilani, R., da Costa, M.B.A., Vieira, E.D., Yoschi, S., Konertz, W., and da Costa, I.A. Comparison of cryopreserved homografts and decellularised porcine heterografts implanted in sheep. Artif Organs **28,** 366, 2004.
27. Dohmen, P.M., da Costa, F., Yoshi, S., Lopes, S.V., da Souza, F.P., Vilani, R., Wouk, A.F., da Costa, M., and Konertz, W. Histological evaluation of tissue engineered heart valves implanted in the juvenile sheep model: is there a need for *in vitro* seeding? J Heart Valve Dis **15,** 823, 2006.
28. Erdbrugger, W., Konertz, W., Dohmen, P.M., Posner, S., Ellerbrok, H., Brodde, O-T., Robenek, H., Modersohn, D., Pruss, A., Holinski, S., Stein-Konertz, M., and Pauli, G. Decellularised xenogeneic heart valves reveal remodeling and growth potential *in vivo*. Tissue Eng **12,** 2059, 2006.
29. Hiemann, N.E., Mani, M., Hubler, M., Meyer, R., Hetzer, R., Thieme, R., and Bethge, C. Complete destruction of a tissue-engineered porcine xenograft in pulmonary valve position after Ross procedure. J Thorac Cardiovasc Surg **139,** e67, 2010.
30. Konertz, W., Angeli, E., Tarusinov, G., Christ, T., Kroll, J., Dohmen, P.M., Krogmann, O., Franzbach, B., Napoleone, C.P., and Gargiulo, G. Right ventricular outflow tract reconstruction with decellularised porcine xenografts in patients with congenital heart disease. J Heart Valve Dis **20,** 341, 2011.
31. Perri, G., Polito, A., Esposito, C., Albanese, S.B., Francalanci, P., Pongiglione, G., and Carotti, A. Early and late failure of tissue engineered pulmonary valve conduits used for right ventricular outflow tract reconstruction in patients with congenital heart disease. Eur J Cardiothorac Surg **41,** 1320, 2012.
32. Cicha, I., Ruffer, A., Cesnjevar, R., Glockler, M., Agaimy, A., Daniel, W.G., Garlichs, C.D., and Dittrich, S. Early obstruction of decellularised xenogenic valves in pediatric patients: involvement of inflammatory and fibroproliferative processes. Cardiovasc Pathol **20,** 222, 2011.
33. Booth, C., Korossis, S., Wilcox, H.E., Watterson, K.G., Kearney, J.N., Fisher, J., and Ingham, E. Tissue engineering a cardiac valve prosthesis I: development and histological characterisation of an acellular porcine scaffold. J Heart Valve Dis **11,** 457, 2002.
34. Korossis, S., Booth, C., Wilcox, H.E., Ingham, E. Kearney, J.N., Watterson, K.G., and Fisher, J. Tissue engineering a cardiac valve prosthesis II: biomechanical characterisation of decellularised porcine heart valves. J Heart Valve Dis **11,** 463, 2002.
35. Wilcox, H.E., Korossis, S.A., Booth, C., Watterson, K.G., Kearney, J.N., Fisher, J., and Ingham, E. Biocompatibility and recellularization potential of an acellular porcine heart valve matrix. J Heart Valve Dis **14,** 228, 2005.
36. Korossis, S.A., Wilcox, H.E., Watterson, K.G., Kearney, J.N., Ingham, E., and Fisher, J. *In vitro* assessment of the functional performance of the decellularised intact porcine aortic root. J Heart Valve Dis **14,** 408, 2005.
37. Brown, B.N., Ratner, B.D., Goodman, S.B., Amar, S., and Badylak, S.F. Macrophage polarisation: An opportunity for improved outcomes in biomaterials and regenerative medicine. Biomaterials **33,** 3792, 2012.
38. Brown, B.N., and Badylak, S.F. Expanded applications, shifting paradigms and an improved understanding of host-biomaterial interactions. Acta Biomater **9,** 4948, 2013.
39. Lech, M., and Anders, H.-J. Macrophages and fibrosis: how resident and infiltrating mononuclear phagocytes orchestrate all phases of tissue injury and repair. Biochim Biophys Acta **1832,** 989, 2013.
40. Iop, L., Bonetti, A., Naso, F., Rizzo, S., Cagnin, S., Bianco, R., Lin, C.D., Martini, P., Poser, H., Franci, P., Lanfranchi, G., Busetto, R., Spina, M., Basso, C., Marchini, M., Ganaglia, A., Ortolani, F., and Gerosa, G. Decellularized allogeneic heart valves demonstrate self-regeneration potential after a long-term preclinical evaluation. PLoS One **9,** e99593, 2014.
41. Leyh, R.G., Wilhelmi, M., Rebe, P., Fischer, S., Kofidis, T., Haverich, A., and Mertsching, H. *In vivo* repopulation of xenogeneic and allogeneic acellular valve matrix conduits in the pulmonary circulation. Ann Thorac Surg **75,** 1457, 2003.
42. Aarnio, P., Harjula, A., Lehtola, A., Sariola, H., and Mattila, S. Polydioxanone and polypropylene suture material in free internal mammary artery graft anastomoses. J Thorac Cardiovasc Surg **96,** 741, 1988.
43. Gersak, B. Presence of calcium in the vessel walls after end-to-end arterial anastomoses with polydioxanone and polypropylene sutures in growing dogs. J Thorac Cardiovasc Surg **106,** 587, 1993.

Address correspondence to:
Eileen Ingham, PhD
Faculty of Biological Sciences
School of Biomedical Sciences
University of Leeds
Leeds LS2 9JT
United Kingdom

E-mail: e.ingham@leeds.ac.uk

Received: January 2, 2014
Accepted: July 23, 2014
Online Publication Date: September 26, 2014